Nonlinear Dynamic Analysis of a Rolling Bearing-Rotor System with an Inner Ring Fault

Huining An[1], Jianwei Lü[2,*],Jiahui Zhang[1]

[1]*Baotou Railway Vocational & Technical College, Baotou 730000, China*
[2]*Hohhot Vocational University of Technology, Hohhot 010070, China*
[*]*Corresponding author: ljwvvs@163.com*

Abstract: *Taking the rolling bearing-rotor system as the research object, this study couples the damage dynamics model of the inner ring of the rolling bearing into the system. Using the numerical integration method, the vibration characteristics of the rolling bearing are investigated in detail. The motion state under specific working conditions is analyzed, and the motion law is revealed. The results show that the fault frequency generated by the bearing defect is related to the bearing type and the system speed.*

Keywords: *rolling bearing; rotor system; inner ring fault*

1. Introduction

In rotating machinery, rolling bearings represent the most critical supporting components, as their dynamic behavior can influence the operational state of the entire system. Furthermore, with the advancement of industrial technology, the requirements for such universal mechanical components as rolling bearings are becoming increasingly demanding. It is essential to not only meet the demands for high precision and high rotational speeds but also to enhance their reliability and extend their service life. This necessitates condition monitoring during the service period of rolling bearings to detect faults at an early stage and ensure the normal operation of equipment. It has been statistically shown that mechanical accidents caused by rolling bearing failures account for 7% of the total incidents. During the operation of rolling bearings, the raceways can develop flaws such as pits, scratches, cracks, and spalling. These defects are the primary factors that disrupt normal bearing vibration and induce faults. Therefore, to mitigate the adverse vibrations caused by bearing faults and improve operational accuracy, it is imperative to implement condition monitoring and fault diagnosis for rolling bearings.

Shabaneh N[1] conducted an in-depth analysis of the nonlinear dynamic characteristics of a rotor shaft system with viscoelastic supported bearings, focusing on the influence of viscoelastic materials on the system's vibration frequency and response. Through free and forced vibration analyses, the study revealed the influence patterns of viscoelastic characteristic parameters on the dynamic behavior of the rotor shaft system. Wang C[2] analyzed the vibration behavior of a 2.2 kW induction motor using a finite element model, calculating the winding and bar currents, magnetic forces, and the dynamic response of the motor structure. The results were validated through numerical calculations and measurements. Widdle Jr RD[3] established two torsional vibration models, one assuming a rigid rotor and the other a flexible rotor. The flexible rotor model allows for more effective transmission of high-frequency vibrations and provides better prediction of the measured output shaft vibration. Holopainen T P[4] investigated the influence of electromechanical interaction on rotor dynamics in squirrel-cage induction motors, focusing on how the unbalanced magnetic pull (UMP) alters the rotor's vibration characteristics. By combining a parametric electromagnetic force model with a three-dimensional finite element structural model, the analysis examined the impact of electromagnetic coupling on the vibration of the rotor system, particularly when the motor's rated speed approaches the rotor's bending critical speed. Sassis[5] developed a numerical model for predicting the vibration of rotating ball bearings with local surface defects. The model accounts for factors such as bearing rotation, load distribution, structural elasticity, oil film characteristics, and the transmission path. Using the developed BEAT software, the vibration response of the bearing to excitations generated by local defects was simulated, yielding realistic results comparable to experimental measurements. Choe HC[6] studied neural pattern recognition for railway wheelset bearing faults based on audible acoustic signals, comparing the effectiveness of FFT (Fast Fourier Transform), CWT (Continuous Wavelet Transform),

and DWT (Discrete Wavelet Transform) features in fault identification. Shaoyi Min[7] proposed a novel method for modeling local surface defects in the dynamic simulation of cylindrical roller bearings. This method considers the characteristics of the defect edges, enabling more accurate capture of bearing vibrations.

2. Faulty Rolling Bearing – Rotor System

2.1 Rolling Bearing Fault Characteristic Frequency

Figure 1 shows a schematic diagram of the rolling bearing dimensions. Here, D is the pitch diameter; d is the ball diameter; T is the contact angle; and N_b is the number of balls. This study selects the JIS6306 rolling bearing as the research object. The calculated parameters for the rolling bearing are as follows:

$D = 104$ mm，$d = 11.9$ mm，$T = 0°$，$Nb = 8$

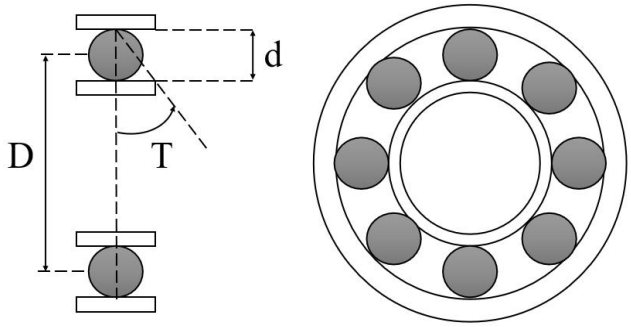

Figure 1 Rolling bearing dimensions

Let the fault frequencies of the rolling bearing outer ring, inner ring, and rolling elements be denoted as f_o, f_i, and f_r, respectively; and let f_R represent the rotational frequency of the rotor. The characteristic fault frequencies of the rolling bearing are shown in Table 1.

Table 1 JIS6306 Rolling Bearing Fault Characteristic Frequencies

Outer Ring	$f_o = \frac{N_b}{2}\left(1-\frac{d}{D}\cos T\right)f_R = 3.0846 f_R$
Inner Ring	$f_i = \frac{N_b}{2}\left(1+\frac{d}{D}\cos T\right)f_R = 4.9154 f_R$
Rolling element	$f_r = \frac{N_b}{2}\left(1-\frac{d}{D}\cos T\right)f_R = 0.385 f_R$

When a fault occurs in a rolling bearing, defects are generated on its working surface. As the rolling elements pass over these defects, variations in clearance are produced.

2.2 Rolling Bearing Inner Ring Fault

2.2.1 Establishment of the Inner Ring Fault Dynamic Model

Figure 2(a) shows a schematic diagram of a defect in the inner ring of a rolling bearing, and Figure 2(b) shows the developed view of the defect. When a local defect occurs at a certain point on the inner ring of a rolling bearing, the passage of a rolling element over this point generates an impact vibration and releases a certain amount of deformation. However, because the bearing inner ring is fixed to the rotating shaft and rotates with the rotor, the contact position where the rolling element enters the defect changes according to the varying position of the defective area. As shown in Figure 2(b), assume the defect formed on the inner ring is a spherical pit. Consequently, the cross-section of this pit represents the defect surface. Let L_i be the diameter of the defect surface, h_i be the defect depth, and u_i be the amount of deformation instantaneously released when the rolling element passes through the defect.

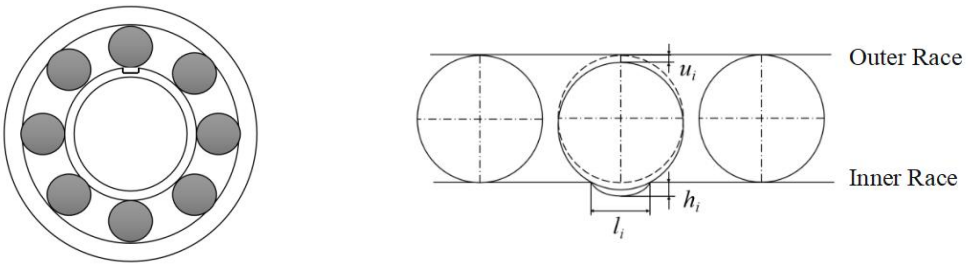

(a) Schematic Diagram of Inner Race Damage

(b) Unrolled Schematic Diagram of Inner Race Damage

Figure 2 Schematic Diagram of Inner Race Damage

The generation of impact vibration when a rolling element passes through an inner ring defect depends on the defect diameter l_i and the defect depth h_i. This is because:

$$h_i = \frac{d}{2} - \sqrt{\left(\frac{d}{2}\right)^2 - \left(\frac{l_i}{2}\right)^2}$$

Solving yields:

$$l_i = 2 \times \sqrt{d \times h_i - \left(h_i\right)^2}$$

When:

$$l_i \le 2 \times \sqrt{d \times h_i - \left(h_i\right)^2}$$

An inner ring fault is necessary to allow the ball to fall into the pit and generate impact vibration.

This paper assumes that all damages to the inner ring of the rolling bearing satisfy the conditions for generating impact vibration. As shown in the figure, after the rolling element enters the defect, the bearing clearance suddenly increases. This may cause the Hertz contact force between the ball that has fallen into the defect and the inner and outer rings to become zero. The deformation amount u_i when the rolling element passes through the defect is:

$$u_i = \frac{d}{2} - \sqrt{\left(\frac{d}{2}\right)^2 - \left(\frac{l_0}{2}\right)^2}$$

However, the position of the inner ring defect varies with the shaft rotation, meaning the location where the rolling element enters the defect also changes. Therefore, the angular position of the i-th ball is defined as:

$$\theta_i = \omega_c t + \frac{2\pi}{N_b}(i-1), \quad (\omega_c \textit{ is the angular velocity of the cage}) 。$$

When the bearing rotates to time t, the angular position of the inner ring defect is: $\theta_{in} = \omega \times t$

The defect size is β_i. Within one full revolution of the rolling element, the bearing clearance changes only when $\theta_{in} \le \theta_i \le \theta_{in} + \beta_i$, that is:

$$u_i = \begin{cases} \dfrac{d}{2} - \sqrt{\left(\dfrac{d}{2}\right)^2 - \left(\dfrac{l_i}{2}\right)^2} & \left(\theta_{in} \le MOD\left(\dfrac{\theta_i}{2\pi}\right) \le \theta_{in} + \beta_i\right) \\ 0 \end{cases}$$

where the damage angle $\beta_i = arcsin(l_i / D_i)$, and D_i is the inner ring diameter.

When a rolling element falls into the defect, it causes a change in the clearance. This variation in clearance leads to a change in the Hertz contact force of the rolling bearing. This section assumes that

the inner ring defect exists only on the right bearing, while the left bearing is fault-free. Therefore, the total Hertz contact force of the bearing in the x and y directions is:

$$f_{ixR} = -\sum_{i=1}^{N_b} k_{bR}[(x_R \cos\theta_i + y_R \sin\theta_i) - \gamma - u_i]_+^{1.5} \cos\theta_i$$

$$f_{iyR} = -\sum_{i=1}^{N_b} k_{bR}[(x_R \cos\theta_i + y_R \sin\theta_i) - \gamma - u_i]_+^{1.5} \sin\theta_i$$

$$f_{xL} = -\sum_{i=1}^{N_b} k_{bL}[(x_L \cos\theta_i + y_L \sin\theta_i) - \gamma]_+^{1.5} \cos\theta_i$$

$$f_{yL} = -\sum_{i=1}^{N_b} k_{bL}[(x_L \cos\theta_2 + y_L \sin\theta_i) - \gamma]_+^{1.5} \sin\theta_i$$

Therefore, the dynamic equation of the rolling bearing with an inner ring defect can be expressed as:

$$\begin{cases} m_R\ddot{x}_R + c_b\dot{x}_R + k\left(x_R - x_p\right) = f_{ixR} \\ m_R\ddot{y}_R + c_b\dot{y}_R + k\left(y_R - y_p\right) = f_{iyR} - m_R g \\ m_p\ddot{x}_p + c_p\dot{x}_p + k\left(x_p - x_R\right) + k\left(x_p - x_L\right) = m_p e\omega^2 \cos\left(\omega t\right) \\ m_p\ddot{y}_p + c_p\dot{y}_p + k\left(y_p - y_R\right) + k\left(y_p - y_L\right) = m_p e\omega^2 \sin\left(\omega t\right) - m_p g \\ m_L\ddot{x}_L + c_b\dot{x}_L + k\left(x_L - x_p\right) = f_{xL} \\ m_L\ddot{y}_L + c_b\dot{y}_L + k\left(y_L - y_p\right) = f_{yL} - m_L g \end{cases}$$

3. Simulation Analysis of Inner Ring Fault

The parameters selected for the rotor system are as follows: eccentricity e = 0.01 mm; stiffness k = 2.5×10^7N/m; clearance γ = 5 μm. The parameters for the inner ring fault are as follows: inner ring defect diameter l_i = 0.5 mm; inner ring defect depth h_i = 1 mm; rolling bearing inner ring diameter D_i = 80.2 mm. The defect is located on the raceway of the inner ring of the right-end bearing.

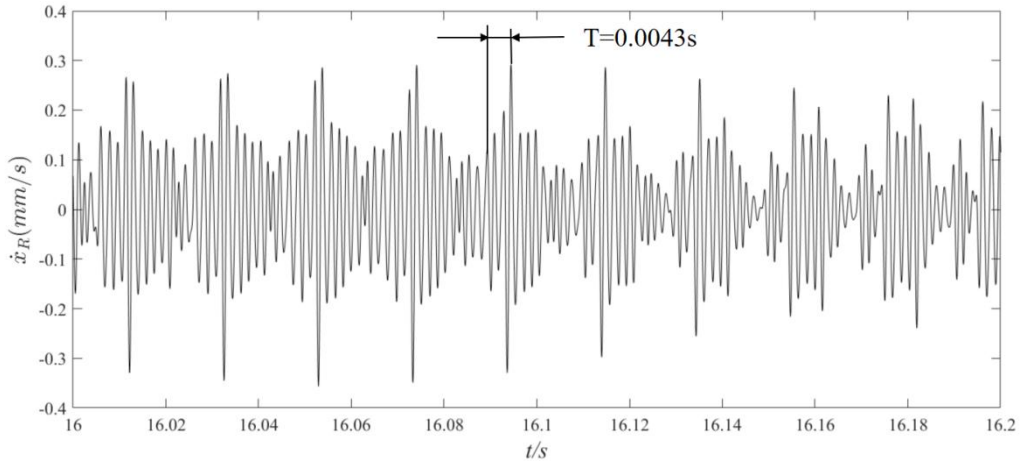

Figure 3 Time History Plot of Velocity $\dot{x}R$

This paper conducts a simulation solution at a rotor speed of ω = 300 rad/s, that is, $f_R \approx 48$ Hz. From Table 1, the characteristic frequency of the inner ring damage is obtained as $f_i = 48 \times 4.9154 \approx 236$ Hz. The simulation results are shown in Figure 3. When a defect exists in the inner ring of the rolling bearing, the vibration impact on the system is relatively complex due to the continuous change in the

position of the inner ring defect. Figure 3 shows the time history of the velocity in the X_R direction of the right rolling bearing.

As shown in Figure 3, when the ball is about to pass through the inner ring defect, an impact force is generated due to the sudden change in clearance, causing a sudden change in the vibration amplitude of the right bearing. After the ball passes through the defect, the bearing system produces a series of decaying vibrations. The figure shows that the impact period of the velocity pulse signal in the X_R direction is T = 0.0043 s, indicating a frequency of approximately 232.6 Hz. This measured value is close to the theoretical characteristic frequency of the inner ring fault, f_i = 236 Hz, thereby validating the model presented in this paper.

Since the position of the inner ring defect changes with the rotation of the shaft, the magnitude of the impact force generated by the inner ring fault is modulated by the rotational frequency. As can be observed from Figure 3, the vibration impact repeats every rotational cycle with an interval frequency of 48 Hz (1/0.021), which equals the rotational frequency. Furthermore, the time history exhibits amplitude modulation characteristics consistent with the rotational frequency, meaning the vibration amplitude of the bearing system also displays periodic variations.

Conclusion

The above analysis demonstrates that when a fault exists in the bearing inner ring, the system generates a larger impact force as the defect diameter increases. The corresponding variation in the total Hertz contact force also differs significantly and is proportional to the defect diameter. Furthermore, the system amplitude increases with the defect diameter, leading to less stable operation. Therefore, for rolling bearings, the diameter of an inner ring defect significantly influences operational stability and is a primary factor affecting the Hertz contact force. Consequently, during the operation of machine tool spindle systems, it is essential to regularly inspect the bearing inner ring for faults such as pitting. By monitoring the system's operational status and comparing it with the simulation results derived from the established model, the operational state of the rolling bearing can be assessed, thereby ensuring the stable operation of the system.

Fund Projects

2025 Research Project of Baotou Railway Vocational & Technical College: "Study on the Influence of Rolling Bearing–Rotor System Vibration on the Operational Stability of High-Speed Trains and Fault Diagnosis Research," Project No.: BTZY202513.

2025 Inner Mongolia Autonomous Region Education Scientific Research "14th Five-Year Plan" Project: "Research on the Innovation Path of Ideological and Political Education in Rail Transit Courses in Universities Empowered by AI," Project No.: NZJGH2025115.

References

[1] Shabaneh N, Jean W Z.. Journal of Vibration and Acoustics, 2003, 125(3): 290—298.
[2] Wang C, Lai J C S. Vibration analysis of an induction motor. Journal of Sound and Vibration, 1999, 224(4): 733—756.
[3] Widdle Jr R D, Krousgrill Jr C M, Sudhoff S D. An induction motor model for high-frequency torsional vibration analysis [J]. Journal of Sound and Vibration, 2006, 290(3): 865—881.
[4] Holopainen T P, Tenhunen A, Arkkio A. Electromechanical interaction in rotor dynamics of cage induction motors. Journal of Sound and Vibration, 2005, 284(3): 733—755.
[5] Sassi S, Badri B, Thomas M. A numerical model to predict damaged bearing vibrations. Journal of Vibration and Control, 2007, 13(11): 1603-1628
[6] Choe HC, Wan Y, Chan AK. Neural pattern identification of railway wheel-bearing faults from audible acoustic signals: Comparison of FFT, CWT, and DWT features. SPIE Proceedings on Wavelet Applications, 1997 (3078): 480-496.
[7] Shaoyi Min, Liu Jing, Ye Jun. A new method to model a localized surface defect in a cylindrical roller-bearing dynamic simulation. Proc IMechE, Part J: Journal of Engineering Tribology, 2014, 228(2): 140-159.